Available online at www.sciencedirect.com

ScienceDirect

Procedia Materials Science 10 (2015) 80 – 89

Procedia Materials Science

www.elsevier.com/locate/procedia

2nd International Conference on Nanomaterials and Technologies (CNT 2014)

Transient MHD free convection flow and heat transfer of nanofluid past an impulsively started vertical porous plate in the presence of viscous dissipation

V. Rajesh[1]*, M. P. Mallesh[2] and O. Anwar Bég[3]

[1, 2] *Department of Engineering Mathematics, GITAM University Hyderabad Campus, Rudraram, Patancheru Mandal, Medak Dist.-502 329, A.P. India.*

[3] *Gort Engovation (Aerospace Engineering Sciences), 15 Southmere Avenue, Bradford,BD7 3NU, England, UK.*

Abstract

A mathematical model is developed for the nanofluid flow and heat transfer due to the impulsive motion of an infinite vertical porous plate in its own plane in the presence of a magnetic field and viscous dissipation. The governing unsteady, coupled, non-linear partial differential equations are transformed into a system of nonlinear ordinary differential equations, with appropriate boundary conditions. A robust Galerkin finite element numerical solution is developed. A range of nanofluids containing nanoparticles of aluminium oxide, copper, titanium oxide and silver with nanoparticle volume fraction ranges less than or equal to 0.04 are considered. The Tiwari-Das nanofluid model is employed. The velocity and temperature profiles as well as the skin friction coefficient and Nusselt number are examined for different parameters such as nanoparticle volume fraction, nanofluid type, magnetic parameter, thermal Grashof number, Eckert number and suction parameter. The present simulations are relevant to magnetic nanomaterials thermal flow processing in the chemical engineering and metallurgy industries.

Peer-review under responsibility of the International Conference on Nanomaterials and Technologies (CNT 2014)

Keywords: Free convection; nanofluids; Galerkin finite element method; MHD; infinite vertical porous plate; transient flow; viscous dissipation; materials processing.

* Corresponding author. Tel.: +91-9441146761

E-mail address: v.rajesh.30@gmail.com

Peer-review under responsibility of the International Conference on Nanomaterials and Technologies (CNT 2014)

doi:10.1016/j.mspro.2015.06.028

Nomenclature

M	Magnetic parameter
Ec	Eckert number
λ	suction parameter
Gr	thermal Grashof number
t	time
T	temperature
U	velocity along x-axis,
ρ	density
μ	dynamic viscosity
β	thermal expansion coefficient
g	acceleration due to gravity,
κ	thermal conductivity
n	empirical shape factor for the nanoparticle
ϕ	nanoparticle volume fraction
ν	kinematic viscosity
subscripts	
nf	nanofluids
f	base fluid
s	solid nanoparticles

1. Introduction

Convectional heat transfer fluids, including oil, water, and ethylene glycol mixture are poor heat transfer fluids. Since the thermal conductivity of these fluids plays an important role in determining the coefficient of heat transfer between the heat transfer medium and the heat transfer surface, numerous methods have been used to improve the thermal conductivity of these fluids by suspending nanometer/micrometer-sized particle materials in liquids. Intensive attention has been directed at numerical simulations of natural convection heat transfer in nanofluids both with and without magnetic fields, and representative studies include Congedo *et al.*(2009). Uddin *et al.*(2014) employed MAPLE symbolic quadrature to study numerically the electromagnetic nanofluid flow in porous media with wall slip and radiation heat transfer effects. Bég *et al.*(2014) applied implicit finite difference methods to analyse the magnetic bio-nanofluid induction flow from a stretching surface with surface tension effects. Rana *et al.* (2013) used a variational finite element method to simulate rotating magnetic nanofluid boundary layer flow, heat and mass transfer from an extruding sheet. Recently Rajesh et al.(2014) presented a mathematical model for the unsteady free convective flow and heat transfer of a viscous nanofluid from a moving vertical cylinder in the presence of thermal radiation. Later Rajesh and Anwar Beg (2014) numerically studied the effects of MHD on the transient free convection flow of a viscous, electrically conducting, and incompressible nanofluid past a moving semi-infinite vertical cylinder with temperature oscillation.

Transient free convection flows under the influence of a magnetic field have attracted the interest of many researchers in view of their applications in modern materials processing where magnetic fields are known to achieve excellent manipulation and control of electrically-conducting materials (Ibrahim and Shankar, 2014). Magnetohydrodynamic (MHD) convection flows also find significant applications in renewable energy devices, including MHD power generators (Chen et. al.2005, Yamaguchi, 2011) as well as nuclear reactor transport processes (Mukhopadhyay, 2011) wherein magnetic field is employed to regulate heat transfer rates. In view of these applications, the present study is proposed to examine the effects of transverse magnetic field on transient free convective flow of nanofluid past an impulsively started infinite vertical porous plate with viscous dissipation. The present study also provides an important benchmark for further simulations of magneto-nanofluid dynamic transport phenomena of relevance to materials processing, with alternative computational algorithms.

2. Mathematical Model

We consider the unsteady laminar two-dimensional boundary layer flow of a viscous incompressible electrically-conducting nanofluid past an impulsively started infinite vertical porous plate in the presence of an applied magnetic field and viscous dissipation effects. The *x*-axis is taken along the plate in the vertically upward direction, and y-axis is taken normal to the plate as shown in Figure 1. The gravitational acceleration *g* acts downward. Initially, both the plate and the nanofluid are stationary at the same temperature T'_∞. They are maintained at this condition for all $t' \le 0$. At time $t' > 0$, the plate is given an impulsive motion in the vertical direction against the gravitational field with the uniform velocity u_0. The temperature on the surface of the plate is raised to $T' = T'_w$, which is thereafter maintained at the same level. A transverse magnetic field of uniform strength B_0 is assumed to be applied normal to the plate. We assume that the effect of the induced magnetic field is negligible, which is valid when the magnetic Reynolds number is small. The Ohmic heating, ionslip and Hall effects are neglected as they are also assumed to be small. As the plate is infinite in extent, the physical variables are functions of y and t' only. The fluid is water based magnetic nanofluid containing different types of nanoparticles: aluminium oxide $\left(Al_2O_3\right)$, copper $\left(Cu\right)$, titanium oxide $\left(TiO_2\right)$ and silver $\left(Ag\right)$. In this study, nanofluids are assumed to behave as single-phase fluids with local thermal equilibrium between the base fluid and the nanoparticles suspended in them so that no slip occurs between them. The thermo-physical properties of the nanoparticles (Oztop and Abu-Nada, 2008) are given in Table 1.

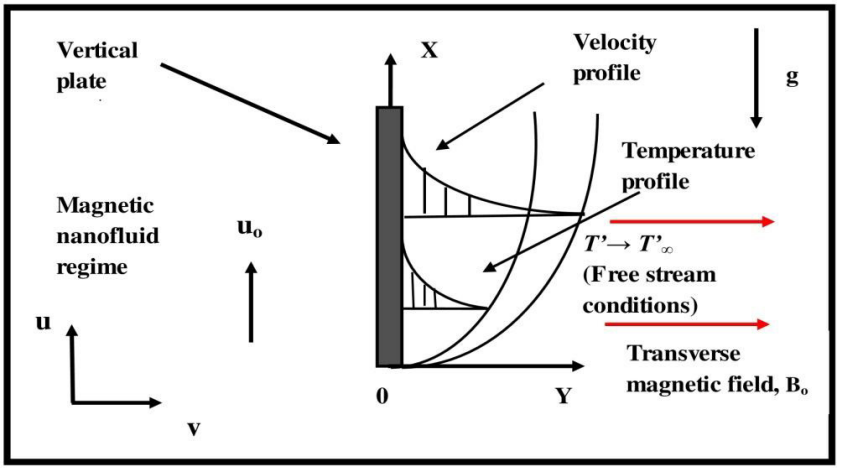

Figure 1: The physical model and coordinate system

Under the above assumptions, and following the nanofluid model proposed by Tiwari and Das (2007), with the usual Boussinesq approximation (Schlichting and Gersten, 2001), the governing equations are:

$$\frac{\partial v}{\partial y} = 0 \tag{1}$$

$$\frac{\partial u}{\partial t'} + v\frac{\partial u}{\partial y} = \nu_{nf}\frac{\partial^2 u}{\partial y^2} + \frac{(\rho\beta)_{nf}}{\rho_{nf}} g\left(T' - T'_\infty\right) - \frac{\sigma B_0^2 u}{\rho_{nf}} \tag{2}$$

$$\frac{\partial T'}{\partial t'}+v\frac{\partial T'}{\partial y}=\frac{\kappa_{nf}}{\left(\rho c_p\right)_{nf}}\frac{\partial^2 T'}{\partial y^2}+\frac{\mu_{nf}}{\left(\rho c_p\right)_{nf}}\left(\frac{\partial u}{\partial y}\right)^2 \tag{3}$$

The initial and boundary conditions are

$$\begin{aligned} &t'\le 0:\ \mathrm{u}=0, \quad \mathrm{T}'=\mathrm{T}'_\infty \quad \text{for all} \quad \mathrm{y}\\ &t'>0:\ \mathrm{u}=\mathrm{u}_0, \quad \mathrm{T}'=\mathrm{T}'_w \quad \text{for} \quad \mathrm{y}=0\\ &\qquad \mathrm{u}\to 0, \quad \mathrm{T}'\to \mathrm{T}'_\infty \quad \text{as} \quad \mathrm{y}\to\infty \end{aligned} \tag{4}$$

Equation (1) gives $v=-v_0\left(v_0>0\right)$ (5)

Where v_0 is the constant suction velocity and the negative sign indicates that it is towards the plate.

For nanofluids, the expressions of density ρ_{nf}, thermal expansion coeffcient $\left(\rho\beta\right)_{nf}$ and heat capacitance $\left(\rho c_p\right)_{nf}$ are given by

$$\begin{aligned} \rho_{nf}&=\left(1-\phi\right)\rho_f+\phi\rho_s\\ \left(\rho\beta\right)_{nf}&=\left(1-\phi\right)\left(\rho\beta\right)_f+\phi\left(\rho\beta\right)_s\\ \left(\rho C_p\right)_{nf}&=\left(1-\phi\right)\left(\rho C_p\right)_f+\phi\left(\rho C_p\right)_s \end{aligned} \tag{6}$$

The effective thermal conductivity of the nanofluid according to Hamilton and Crosser (1962) model is given by

$$\frac{\kappa_{eff}}{\kappa_f}=\frac{\kappa_s+\left(n-1\right)\kappa_f-\left(n-1\right)\phi\left(\kappa_f-\kappa_s\right)}{\kappa_s+\left(n-1\right)\kappa_f+\phi\left(\kappa_f-\kappa_s\right)} \tag{7}$$

Where n is the empirical shape factor for the nanoparticle. In particular, n=3 for spherical shaped nanoparticles and n=3/2 for cylindrical ones.

Table 1. Thermo-physical properties of water and nanoparticles

	H_2O	Al_2O_3	Cu	TiO_2	Ag
$\rho\left(Kg\,m^{-3}\right)$	997.1	3970	8933	4250	10500
$C_p\left(J\,Kg^{-1}K^{-1}\right)$	4179	765	385	686.2	235
$\kappa\left(Wm^{-1}K^{-1}\right)$	0.613	40	401	8.9528	429
$\beta\times10^{-5}\left(K^{-1}\right)$	21	0.85	1.67	0.9	1.89

Introducing the following non dimensional variables in equations (2) and (3):

$$U=\frac{u}{u_0},\ t=\frac{t'u_0^2}{\nu_f},\ Y=\frac{yu_0}{\nu_f},\ T=\frac{T'-T'_\infty}{T'_w-T'_\infty},\ G_r=\frac{g\beta_f\nu_f\left(T'_w-T'_\infty\right)}{u_0^3},\ P_r=\frac{\nu_f}{\alpha_f}=\frac{\left(\mu c_p\right)_f}{k_f},$$

$$M=\frac{\sigma B_0^2 \nu_f}{\rho_f u_0^2},\ \lambda=-\frac{\nu}{u_0},\ E_c=\frac{u_0^2}{\left(c_p\right)_f\left(T_w'-T_\infty'\right)} \tag{8}$$

The governing equations reduces to

$$\frac{\partial U}{\partial t}-\lambda\frac{\partial U}{\partial Y}=\frac{1}{\left(1-\phi\right)^{2.5}}\frac{1}{\left(1-\phi+\phi\left(\frac{\rho_s}{\rho_f}\right)\right)}\frac{\partial^2 U}{\partial Y^2}+\frac{\left(1-\phi+\phi\frac{\left(\rho\beta\right)_s}{\left(\rho\beta\right)_f}\right)}{\left(1-\phi+\phi\frac{\left(\rho\right)_s}{\left(\rho\right)_f}\right)}GrT-\frac{1}{\left(1-\phi+\phi\left(\frac{\rho_s}{\rho_f}\right)\right)}MU \tag{9}$$

$$\frac{\partial T}{\partial t}-\lambda\frac{\partial T}{\partial Y}=\frac{k_{nf}}{k_f}\frac{1}{\left(1-\phi+\phi\frac{\left(\rho c_p\right)_s}{\left(\rho c_p\right)_f}\right)}\frac{1}{P_r}\frac{\partial^2 T}{\partial Y^2}+\frac{1}{\left(1-\phi\right)^{2.5}}\frac{1}{\left(1-\phi+\phi\frac{\left(\rho c_p\right)_s}{\left(\rho c_p\right)_f}\right)}E_c\left(\frac{\partial U}{\partial Y}\right)^2 \tag{10}$$

The corresponding dimensionless boundary conditions are:

$$\begin{aligned} &t\le 0:\ \mathrm{U}=0,\quad T=0\quad \text{for all}\quad \mathrm{Y}\\ &t>0:\ \mathrm{U}=1,\quad T=1\quad \text{at}\quad \mathrm{Y}=0\\ &\quad\ \mathrm{U}\to 0,\quad T\to 0\quad \text{as}\quad \mathrm{Y}\to\infty \end{aligned} \tag{11}$$

Let $E_1=\frac{1}{\left(1-\phi\right)^{2.5}}\frac{1}{\left(1-\phi+\phi\left(\frac{\rho_s}{\rho_f}\right)\right)}$, $E_2=\frac{\left(1-\phi+\phi\frac{\left(\rho\beta\right)_s}{\left(\rho\beta\right)_f}\right)}{\left(1-\phi+\phi\frac{\left(\rho\right)_s}{\left(\rho\right)_f}\right)}$, $E_3=\frac{1}{\left(1-\phi+\phi\left(\frac{\rho_s}{\rho_f}\right)\right)}$,

$$E_4=\frac{k_{nf}}{k_f}\frac{1}{\left(1-\phi+\phi\frac{\left(\rho c_p\right)_s}{\left(\rho c_p\right)_f}\right)},\ E_5=\frac{1}{\left(1-\phi\right)^{2.5}}\frac{1}{\left(1-\phi+\phi\frac{\left(\rho c_p\right)_s}{\left(\rho c_p\right)_f}\right)}$$

Now the equations (8) and (10) in terms of $E_1, E_2, E_3, E_4, and\ E_5$ are

$$\frac{\partial U}{\partial t}-\lambda\frac{\partial U}{\partial Y}=E_1\frac{\partial^2 U}{\partial Y^2}+E_2GrT-E_3MU \tag{12}$$

$$\frac{\partial T}{\partial t}-\lambda\frac{\partial T}{\partial Y}=E_4\frac{1}{P_r}\frac{\partial^2 T}{\partial Y^2}+E_cE_5\left(\frac{\partial U}{\partial Y}\right)^2 \tag{13}$$

3. Numerical solutions to Boundary value problem

A robust Galerkin finite element method has been used to solve the governing non-dimensional equations (12) and (13) under the initial and boundary conditions (11). The fundamental steps comprising the method are explained by Rajesh (2014). Further details of FEM are provided by Reddy (1985) and Bathe (1996).

Applying the Galerkin finite element method for equations (12) and (13) over the element (e) $\left(Y_j \le Y \le Y_k\right)$ yields

$$\int_{Y_j}^{Y_k} N^{(e)^T}\left(E_1\frac{\partial^2 U^{(e)}}{\partial Y^2}+\lambda\frac{\partial U^{(e)}}{\partial Y}-\frac{\partial U^{(e)}}{\partial t}+E_2 GrT-E_3 MU^{(e)}\right)dY=0 \tag{14}$$

$$\int_{Y_j}^{Y_k} N^{(e)^T}\left(E_4\frac{1}{\Pr}\frac{\partial^2 T^{(e)}}{\partial Y^2}+\lambda\frac{\partial T^{(e)}}{\partial Y}-\frac{\partial T^{(e)}}{\partial t}+E_c E_5\left(\frac{\partial U}{\partial Y}\right)^2\right)dY=0 \tag{15}$$

Let the linear, piecewise approximation solution be

$$U^e=N_j\left(Y\right)U_j\left(t\right)+N_k\left(Y\right)U_k\left(t\right)=N_jU_j+N_kU_k \tag{16}$$

$$T^e=N_j\left(Y\right)T_j\left(t\right)+N_k\left(Y\right)T_k\left(t\right)=N_jT_j+N_kT_k \tag{17}$$

Where

$$N_j=\frac{Y_k-Y}{Y_k-Y_j},\ N_k=\frac{Y-Y_j}{Y_k-Y_j},\ N^{(e)^T}=\begin{bmatrix}N_j & N_k\end{bmatrix}^T=\begin{bmatrix}N_j\\ N_k\end{bmatrix} \tag{18}$$

The solution of the assembled system of equations is obtained using the Thomas algorithm (Carnahan et. al., 1969) for velocity and temperature. For computational purposes, the coordinate y is varied from 0 to $Y_{\max}=16$, where $Y_{\max}$ represents infinity i.e. external to the momentum and energy boundary layers. After experimenting with a few sets of mesh sizes to access grid independence, the time and spatial step sizes $\Delta t=0.01$ and $\Delta Y=0.2$ were found to give accurate results. Also, Computations were carried out on a Dell Laptop computer using MATLAB R2009a. In order to prove the convergence and stability of the Galerkin finite element method, the same Matlab program was run with slightly modified values of the mesh distance in the Y- and t-directions, i.e. **h** and **k** and no significant change was observed in the values of U and T. Mesh independence of solutions was therefore achieved with excellent stability and convergence.

Table 2. Thermal conductivity and dynamic viscosity for spherical shaped nanoparticles

Model	Shape of nanoparticles	Thermal conductivity	Dynamic viscosity
I	Spherical	$\frac{\kappa_{nf}}{\kappa_f}=\frac{\kappa_s+2\kappa_f-2\phi\left(\kappa_f-\kappa_s\right)}{\kappa_s+2\kappa_f+\phi\left(\kappa_f-\kappa_s\right)}$	$\mu_{nf}=\frac{\mu_f}{\left(1-\phi\right)^{2.5}}$
II	Spherical	$\frac{\kappa_{nf}}{\kappa_f}=\frac{\kappa_s+2\kappa_f-2\phi\left(\kappa_f-\kappa_s\right)}{\kappa_s+2\kappa_f+\phi\left(\kappa_f-\kappa_s\right)}$	$\mu_{nf}=\mu_f\left(1+7.3\phi+123\phi^2\right)$

In materials processing problems, characteristics at the wall are important, for example the skin friction coefficient C_f and the Nusselt number Nu, which are defined in non dimensional form respectively, as follows:

The skin friction coefficient $C_f = \frac{1}{(1-\phi)^{2.5}} \left(\frac{\partial U}{\partial Y} \right)_{Y=0}$ (19)

and The Nusselt number $Nu = -\frac{\kappa_{nf}}{\kappa_f} \left(\frac{\partial T}{\partial Y} \right)_{Y=0}$ (20)

The derivatives involved in Equations (19) and (20) are evaluated using five-point approximation formula.

4. Results and Discussion

To get the physical significance of the problem, the numerical values of velocity and temperature have been computed within the boundary layer for different values of Magnetic parameter (*M*), thermal Grashof number (Gr), nanoparticle volume fraction (ϕ), Eckert number (Ec), Suction parameter (λ) and time (t). In this study, the nanoparticle volume fraction is considered in the range of $0 \le \phi \le 0.04$, as sedimentation takes place when the nanoparticle volume fraction exceeds 8%. Also, we consider spherical nanoparticles with thermal conductivity and dynamic viscosity shown in Model I in Table 2. The Prandtl number, *Pr* of the base fluid is kept constant at 6.2. When $\varphi = 0$ the model contracts to the governing equations for a regular viscous fluid i.e. nanoscale characteristics are eliminated.

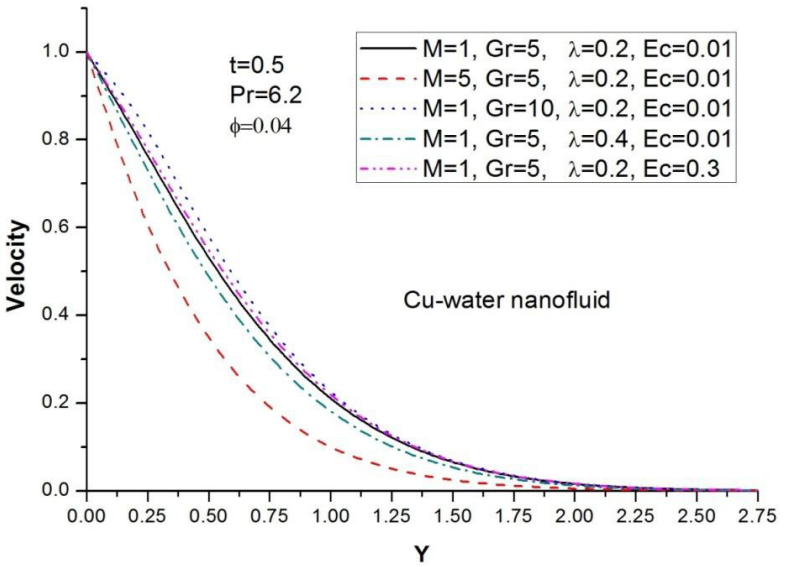

Figure 2. Transient velocity profiles for different M, Gr, Ec, λ

The transient velocity and temperature profiles Cu-water nanofluid for different values of M, Gr, Ec and λ are presented in Figures 2 and 3 respectively. It is found that the velocity of Cu-water nanofluid decreases with the increase in M. The reason behind this phenomenon is that application of magnetic field to an electrically conducting nanofluid gives rise to a resistive type force called the Lorentz force. This force has the tendency to slow down the motion of the nanofluid in the boundary layer. But the effect of M on the temperature of the Cu-water nanofluid is negligible. The parameter Gr signifies the relative influence of thermal buoyancy force and viscous force in the boundary layer regime. It is also seen that the velocity of Cu-water nanofluid increases with the increase in Gr. This means that the buoyancy force accelerates velocity field. But the effect of Gr is found to be negligible on the temperature field of Cu-water nanofluid. The Eckert number, *Ec*, expresses the relationship between the kinetic energy in the flow and the enthalpy. It embodies the conversion of kinetic energy into internal energy by work done against the viscous fluid stresses, and this energy is dissipated as heat. Greater viscous dissipative heat therefore causes a rise in the temperature as well as the velocity. Moreover, it is observed in figures that the velocity and

temperature decrease with an increase in λ . Tables 3 and 4 present the effects of ϕ and t on the transient velocity and temperature of Cu-water nanofluid when Pr = 6.2, Gr = 5, M=1, $\lambda = 0.2$, Ec=0.01.

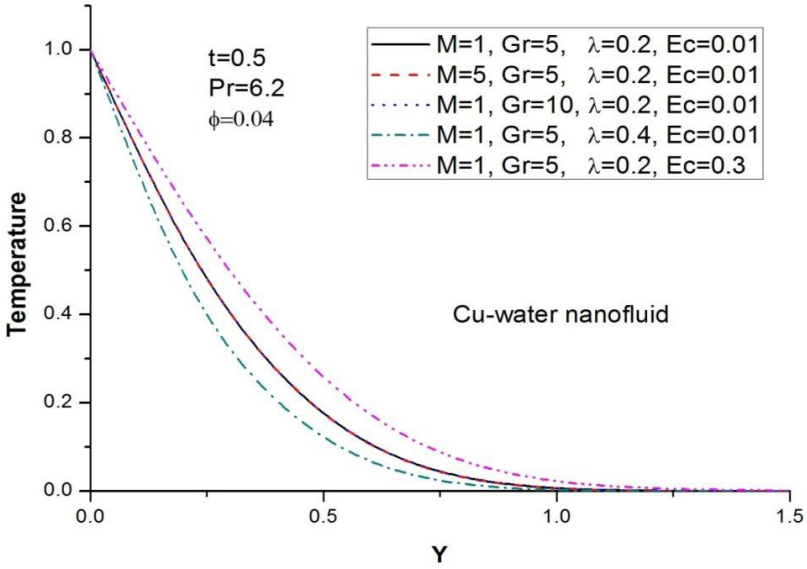

Figure 3. Transient temperature profiles for different M, Gr, Ec, λ

The velocity and temperature profiles of Cu -water nanofluid are found to increase with a rise in time. It is also found that, the temperature increases with an increase in ϕ . This is due to the fact that an increase in ϕ leads to an increase in the thermal conductivity of the nanofluid. However an increase in ϕ leads to the decrease in velocity of Cu -water nanofluid.

Table 3. Transient velocity of Cu-water nanofluid for different ϕ and t

	t=0.5			t=1		
Y	$\phi = 0$	$\phi = 0.02$	$\phi = 0.04$	$\phi = 0$	$\phi = 0.02$	$\phi = 0.04$
0	1	1	1	1	1	1
0.4	0.6376	0.6286	0.6209	0.7288	0.7252	0.7219
0.8	0.3391	0.3256	0.3145	0.4587	0.4533	0.4486
1	0.2363	0.2224	0.211	0.3521	0.3456	0.3401
1.4	0.1056	0.0941	0.0851	0.1987	0.191	0.1845
1.8	0.0417	0.0346	0.0293	0.107	0.0997	0.0937
2	0.0249	0.0197	0.0161	0.0772	0.0705	0.0651
2.4	0.0079	0.0057	0.0042	0.0386	0.0337	0.0299
2.8	0.0022	0.0013	0.0009	0.0182	0.0151	0.0127
3	0.0011	0.0006	0.0004	0.0122	0.0098	0.0081
3.4	0.0002	0.0001	0.0001	0.0053	0.0039	0.003
3.8	0	0	0	0.0021	0.0014	0.001
4	0	0	0	0.0013	0.0009	0.0006

Table 4. Transient temperature of Cu-water nanofluid for different ϕ and t

	t=0.5			t=1		
Y	$\phi = 0$	$\phi = 0.02$	$\phi = 0.04$	$\phi = 0$	$\phi = 0.02$	$\phi = 0.04$
0	1	1	1	1	1	1
0.2	0.5413	0.5558	0.5697	0.6318	0.6449	0.6573
0.4	0.2408	0.2575	0.2741	0.366	0.3834	0.4004
0.6	0.0834	0.095	0.107	0.1919	0.2078	0.2238
0.8	0.0204	0.0259	0.032	0.0898	0.1015	0.1136
1	0.0028	0.0044	0.0065	0.037	0.0441	0.0518
1.2	0	0.0002	0.0006	0.0132	0.0168	0.0209
1.4	0	0.0001	0.0001	0.004	0.0055	0.0074
1.6	0	0	0	0.001	0.0015	0.0023
1.8	0	0	0	0.0002	0.0004	0.0006
2	0	0	0	0.0001	0.0001	0.0001

Table 5. Values of Skin friction coefficient for different types of nanofluids when Pr = 6.2.

M	Gr	λ	Ec	ϕ	t	Ag -water	Cu -water	TiO_2 -water	Al_2O_3 -water
1	5	0.2	0.01	0.04	0.5	-0.9786	-0.9607	-0.8999	-0.8925
5	5	0.2	0.01	0.04	0.5	-2.0944	-2.0888	-2.0683	-2.0642
10	5	0.2	0.01	0.04	0.5	-3.0957	-3.0932	-3.0814	-3.0783
1	10	0.2	0.01	0.04	0.5	-0.4850	-0.4716	-0.4176	-0.4067
1	15	0.2	0.01	0.04	0.5	0.0089	0.0177	0.0649	0.0792
1	5	0.3	0.01	0.04	0.5	-1.0839	-1.0626	-0.9920	-0.9836
1	5	0.4	0.01	0.04	0.5	-1.1931	-1.1682	-1.0868	-1.0775
1	5	0.2	0.001	0.04	0.5	-0.9811	-0.9632	-0.9024	-0.8949
1	5	0.2	0.01	0.02	0.5	-0.8891	-0.8801	-0.8500	-0.8463
1	5	0.2	0.01	0	0.5	-0.8027	-0.8027	-0.8027	-0.8027
1	5	0.2	0.01	0.04	1	-0.6307	-0.6231	-0.5921	-0.5853
1	5	0.2	0.01	0.04	1.5	-0.4677	-0.4653	-0.4487	-0.4420

Table 6. Values of Nusselt number for different types of nanofluids when Pr = 6.2.

M	Gr	λ	Ec	ϕ	t	Ag -water	Cu -water	TiO_2 -water	Al_2O_3 -water
1	5	0.2	0.01	0.04	0.5	2.7482	2.7659	2.7390	2.7564
5	5	0.2	0.01	0.04	0.5	2.7404	2.7578	2.7297	2.7470
10	5	0.2	0.01	0.04	0.5	2.7367	2.7539	2.7253	2.7426
1	10	0.2	0.01	0.04	0.5	2.7486	2.7664	2.7395	2.7570
1	15	0.2	0.01	0.04	0.5	2.7490	2.7668	2.7400	2.7576
1	5	0.3	0.01	0.04	0.5	3.1410	3.1630	3.1351	3.1522
1	5	0.4	0.01	0.04	0.5	3.5641	3.5909	3.5620	3.5785
1	5	0.2	0.001	0.04	0.5	2.7721	2.7892	2.7605	2.7778
1	5	0.2	0.01	0.02	0.5	2.7102	2.7190	2.7057	2.7143
1	5	0.2	0.01	0	0.5	2.6731	2.6731	2.6731	2.6731
1	5	0.2	0.01	0.04	1	2.1525	2.1670	2.1468	2.1594
1	5	0.2	0.01	0.04	1.5	1.8996	1.9129	1.8958	1.9061

The Values of Skin friction coefficient and Nusselt number for different types of nanofluids when Pr = 6.2 are presented in Tables 5 and 6 respectively. It is found that skin friction coefficient for all nanofluids decreases with increasing M, λ , ϕ , but it increases with increasing Gr, Ec and t. From tables it is also found that Nusselt number for all nanofluids decreases with increasing M, Ec, t, but it increases with increasing Gr, λ and ϕ . Moreover Cu -water nanofluid attains an enhanced heat transfer rate when compared with the other nanofluids and Ag -water nanofluid achieves the minimum skin friction coefficient at surface relative to the other nanofluids.

5. Conclusions

This paper investigated transient MHD free convection flow and heat transfer of nanofluid past an impulsively started vertical porous plate in the presence of viscous dissipation. Numerical calculations are carried out for various values of the dimensionless parameters. The effects of various physical parameters on the nanofluid flow and heat transfer characteristics were examined. The present computations have shown that the rate of heat transfer decreased with the increase in Magnetic parameter and Eckert number. But as Suction parameter and nanoparticle volume fraction increased, the rate of heat transfer increased for all nanofluids. Choosing copper as nanoparticle leads to the enhanced heat transfer rate compared to the other nanofluids.

References

Anwar Bég, O., Ferdows, M., Islam, S., Nazrul Islam, M., 2014. Numerical simulation of Marangoni magnetohydrodynamic bio-nanofluid convection from a non-isothermal surface with magnetic induction effects: a bio-nanomaterial manufacturing transport model. *J. Mechanics Medicine Biology* 14 (3), 1450039.1-1450039.32.

Bathe, K.J., 1996. Finite Element Procedures. Prentice-Hall, Upper Saddle River, NJ.

Carnahan, B., Luther, H.A., Wilkes, J.O., 1969. Applied numerical methods. New York, John Wiley & Sons.

Chen, J., Tyagi, S.K., Kaushik, S.C., Tiwari, V., Wu, C., 2005. Effects of several major irreversibilities on the thermodynamic performance of a regenerative MHD power cycle. *ASME J. Energy Resour. Technol* 127(2), 103-118.

Congedo, P.M., Collura, S., Congedo, P.M., 2009. Modeling and analysis of natural convection heat transfer in nanofluids. Proc. ASME Summer Heat Transfer Conf. 3, 569–579.

Hamilton, R.L., Crosser, O.K., 1962. Thermal conductivity of heterogeneous two component system. *Ind. &Eng. Chemistry Fundamentals 1 (1),* 187-191.

Ibrahim, W., Shanker, B., 2014. Magnetohydrodynamic boundary layer flow and heat Transfer of a nanofluid over non-isothermal stretching sheet. *ASME J. Heat Transfer* 136 (5), 051701-051701-9.

Mukhopadhyay, S., 2011. Heat transfer analysis for unsteady MHD flow past a non-isothermal stretching surface. *Nuclear Engineering and Design* 241 (12), 4835-4839.

Oztop, H.F., Abu-Nada, E., 2008. Numerical study of natural convection in partially heated rectangular enclosures filled with nanofluids. *Int. J. Heat Fluid flow 29,* 1326-1336.

Rajesh, V., Anwar Beg, O., Mallesh, M.P., 2014. Transient nanofluid flow and heat transfer from a moving vertical cylinder in the presence of thermal radiation: Numerical study. Proceedings of the Institution of Mechanical Engineers, Part N: Journal of Nanoengineering and Nanosystems, September 5, 2014. Doi: 10.1177/1740349914548712.

Rajesh, V., Anwar Beg, O., 2014. MHD transient nanofluid flow and heat transfer from a moving vertical cylinder with temperature oscillation. Computational thermal sciences 6(5), 439-450.

Rajesh, V., Chamkha, Ali J., 2014.Unsteady convective flow past an exponentially accelerated infinite vertical porous plate with Newtonian heating and viscous dissipation. International Journal of Numerical Methods for Heat & Fluid Flow 24(5), 1109-1123.

Rana, P., Bhargava, R., Anwar Bég, O., 2013. Finite element simulation of unsteady magnetohydrodynamic transport phenomena on a stretching sheet in a rotating nanofluid. *Proc. IMechE- Part N; J. Nanoengineering and Nanosystems* 227 (2), 77-99.

Reddy, J.N., 1985. An Introduction to the Finite Element Method. McGraw-Hill, New York, NY.

Schlichting, H., Gersten, K., 2001. *Boundary Layer Theory.* 8th ed., Springer-Verlag, New York, USA.

Tiwari, R.K., Das, M.K., 2007. Heat transfer augmentation in a two-sided lid-driven differentially-heated square cavity utilizing nanofluids. *Int. J. Heat and Mass Transf 50(*9-10), 2002-2018.

Uddin, M.J., Anwar Bég, O., Ismail Ahmad Izani, Md., 2014. Mathematical modelling of radiative hydromagnetic thermo-solutal nanofluid convection slip flow in saturated porous media. *Math. Prob. Engineering,* Article ID: 179172, 11 pages, doi.org/10.1155/2014/179172.

Yamaguchi, H., Niu, X.D., Zhang, X.R.,.2011.Investigation on a low-melting-point gallium alloy MHD power generator. *Int. J. Energy Research* 35 (10), 209–220.